Regular Article

PHYSICAL CHEMISTRY RESEARCH
Published by the
Iranian Chemical Society
www.physchemres.org
info@physchemres.org

Phys. Chem. Res., Vol. 7, No. 3, 561-579, September 2019
DOI: 10.22036/pcr.2019.183077.1624

Tacrine-Flavonoid Quercetin Hybride as a MTDL Ligand against Alzheimer's Disease with Metal Chelating and AChE, BChE, AChE-induced Aβ Aggregation Inhibition Properties: A Computational Study

R. Habibpour[a,*], M. Eslami[b], P. Amani[a] and S. Bagheri Novir[c]

[a]*Department of Chemical Technologies, Iranian Research Organization for Science and Technology (IROST), Tehran, Iran*

[b]*Pharmaceutical Science Research Center, Shiraz University of Medical Science, Shiraz, Iran*

[c]*Department of Pharmaceutical Chemistry, Faculty of Pharmaceutical Chemistry, Tehran Medical Sciences, Islamic Azad University, Tehran, Iran*

(Received 1 May 2019, Accepted 11 August 2019)

AChE is an enzyme that is predominate in a healthy brain, while BChE is considered to play a minor role in regulating the levels of ACh (memory molecule) in the brain. In addition to setting the ACh level, these two enzymes also facilitate Aβ aggregation by forming stable complexes and participate in the abnormal phosphorylation of the tau protein, which also contribute to the development of Alzheimer's disease (AD). Trace elements including Zn^{2+}, Cu^{2+} and Fe^{2+} are found in the brain plaques of Alzheimer's patients. This study employed tacrine as an efficient inhibitor of cholinesterase and quercetin as a natural metal chelating agent to design a new multi-target-directed ligand, which has been named Tac-Quer. The chelating properties of this ligand have been studied by quantum calculations. The Tac-Quer/Metal binding energies for Zn^{2+}, Cu^{2+} and Fe^{2+} are -939.08, -917.62 and -694.103 kcal mol^{-1}, respectively. The cholinesterase enzyme inhibitory activity of the Tac-Quer ligand has been evaluated *via* molecular dynamic simulations. The free energies for the AChE/Tac-Quer and BChE/Tac-Quer complexes are -17.17 and -29.16 kcal mol^{-1}, respectively. Based on the results, Tac-Quer is introduced as a potent multi-target-directed ligand that can be recognized as a promising treatment for AD.

Keywords: Alzheimer's disease, Tacrine, Quercetin, Docking, Molecular dynamics

INTRODUCTION

Alzheimer's disease (AD) is one of the most common types of neurodegenerative diseases that changes the structure and chemistry of the brain leading to the death of brain cells. AD typically affects people over 65, and its occurrence is expected to increase as the world's population ages. It is estimated that by 2050, more than one percent of the population (one in every 85 people) will live with AD [1]. Thus, it is essential to treat and modify the disease by preventing, delaying or slowing the onset and progression of the disease. The multiple pathological features of AD have made drug designing difficult [2,3]. There is a general agreement that successful treatment will rely on using multi-target-directed ligands (MTDL) to control several pathogens simultaneously [4-6]. There are several theories about AD pathogenesis, with the following ones being the most important: cholinergic neurons damage, unusual deposit of amyloid beta (Aβ) protein in the space in between two neurons, formation of tau proteins twisted fibers inside neurons (neurofibrillary tangles-NFTs), and oxidative stress and free radical formation [7-9].

According to the cholinergic neuron damage theories of AD, damage to the cholinergic neurons leads to a decrease in the acetylcholine (ACh) value. ACh is an important agent in physiological processes such as attention, learning, memory and motivation, wakefulness and sleep, and pain sensation. This neurotransmitter is synthesized in cholinergic neurons from choline and acetyl-coenzymeA using an enzyme called choline acetyltransferase (ChAT)

*Corresponding author. E-mail: Habibpour@irost.ir

(Choline + Acetyl Coenzyme A ⇆ Acetylcholine + Coenzyme A) and also used by cholinergic neurons. Therefore, maintaining its balance in the brain is very important [10]. It is estimated that a 90% loss of ACh occurs in the brain of an Alzheimer's patient.

Cholinesterase (ChE) is an enzyme that hydrolyses ACh to choline and acetic acid reducing the ACh level. It is noteworthy that this enzyme facilitates Aβ aggregation by forming stable complexes and participates in the abnormal phosphorylation of the tau protein [11]. There are two types of ChE, namely acetylcholinesterase (AChE) and butyrylcholinesterase (BChE). These two enzymes differ from each other due to their different tendencies toward substrates. AChE hydrolyses acetylcholine quickly, while BChE rapidly hydrolyses butyrylcholine. The AChE is an α/β hydrolase fold protein composed of 537 amino acids. On the other hand, the neurotransmitter ACh involves an acetoxy group, an ethylene bridge, and a quaternary ammonium cation. AChE interacts with the quaternary ammonium cation of ACh by means of its own 14 aromatic residues that line the deep (20 Å) and narrow (5 Å) gorges. This interaction is a cation-π interaction and leads the ACh down to the catalytic triad.

AChE and BChE have three major sites: the peripheral active site (PAS), the catalytic anionic site (CAS) and the catalytic triad. Deep and narrow gorges actually form the catalytic sites of both AChE and BChE where the hydrolysis reaction occurs. The PAS, as a transitional active site of both AChE and BChE, is attracted to the ammonium cation of ACh in the first step. In the second step, the CAS interacts with the ammonium cation in order to capture the ACh in an appropriate conformation for hydrolysis. In the last step, the hydrolysis of ACh into acetate and choline is carried out by the catalytic triad as the AChE active site. The PAS site of the AChE is rich in aromatic amino acids (Tyr70, Asp72, Tyr121, Trp279 and Tyr334), thus providing a more capacious site in this enzyme for trapping ACh; the PAS site of the BChE includes Asp70 and Tyr332 residues [12-15].

In addition to ACh hydrolysis, the interactions of Aβ monomers with the PAS and the formation of Aβ plaques (AChE-induced Aβ aggregation) must also be controlled because it is toxic for the brain. Therefore, simultaneous containment of both the active and peripheral anionic sites is essential [16-17]. In addition, some studies have shown that the Aβ plaques, in addition to Aβ peptides, have a trace amount of metal ions such as Zn^{2+}, Cu^{2+} and Fe^{2+}. Some of these studies have identified copper ions as the most relevant metal ions involved in the plaque formation [18-19]. Metal ion redox properties play an important role in the formation of reactive oxygen species (ROS), which is a key factor in Aβ toxicity toward neurons. Accordingly, metal targeting strategies seems to be effective methods in the treatment of AD [21,22].

The first FDA-approved drug for AD is tacrine (1,2,3,4-tetrahydroacridin-9-amine) [23]. Due to the hepatotoxicity of tacrine, its clinical use has been restricted. Nevertheless, its high ligand efficiency (LE) has led to its extensive use for MTDLs designing [24]. In order to widen its biological activities for other relevant roles (antioxidant, metal depletion) in the enhancement of controlling other important AD targets, many chemical modifications have been performed. These modifications include functionalization, attachment and incorporation, or even a combination. Moreover, the structure of tacrine dimers has been widely used as a scaffold to design novel MTDLs. The dimer bis(7)tacrine exhibits a better AChE-induced Aβ aggregation beyond the simple AChE inhibition (it has a 1000 times higher AChE inhibition potency than tacrine) due to its dual site binding to PAS and CAS [25,26].

Many theoretical and experimental investigations have been carried out to introduce the novel hybrid molecules of tacrine and other pharmacophores as multi-targeted ligands against Alzheimer's disease: tacrine-hydroxyphenyl-benzimidazole hybrids [27], tacrine-benzyl quinolone carboxylic acid [28], xanomeline-tacrine [29], vilazodone-tacrine, tacrine-ferulic acid [30,31], tacrine-coumarin [32,33], tacrine-huperzine A [34], tacrine-trolox [35], tacrine-scutellarin [36] and vilazodone-tacrine [37,38].

Quercetin (2-(3,4-dihydroxyphenyl)-3,5,7-trihydroxy-chromen-4-one) is a polyphenolic flavonoid mainly found in fruits, vegetables, and cereals [39]. Leopoldini *et al.* [40] investigated iron chelation by quercetin. They showed that quercetin could well chelate iron(II) preventing its participation in the Fenton reaction. Based on the results of experimental studies, all beneficial effects of quercetin on human health are related to its antioxidant properties [41-45].

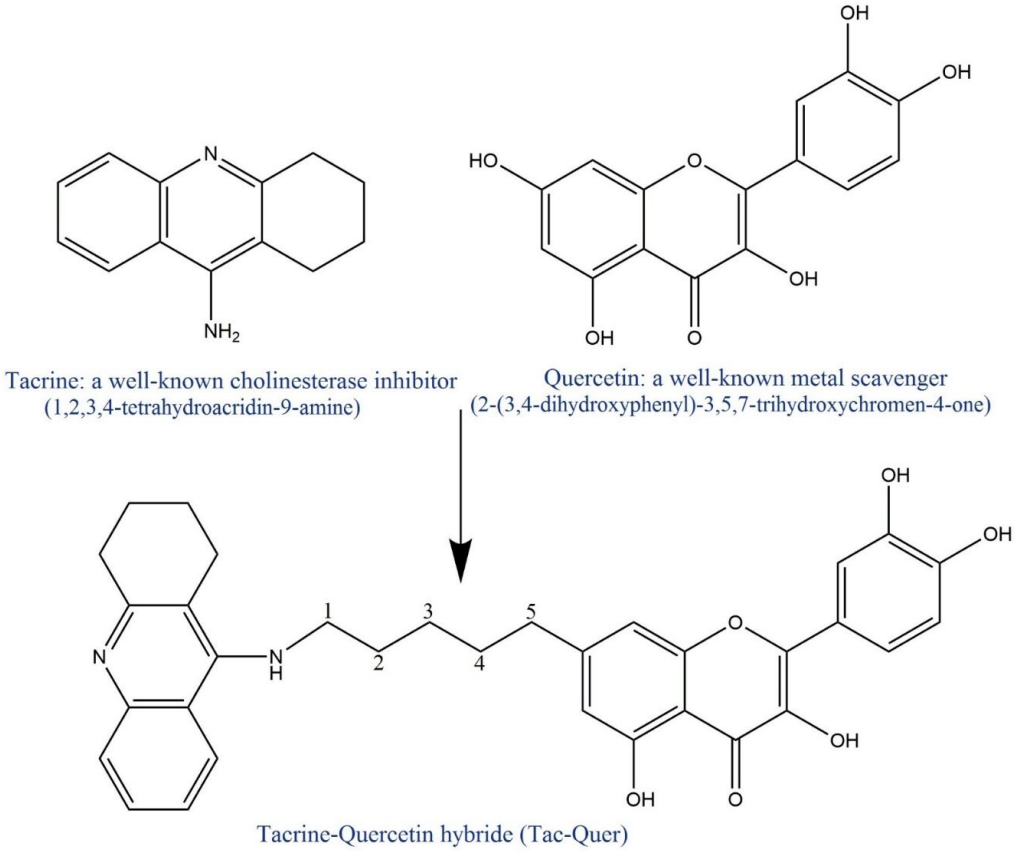

Fig. 1. Chemical structures of tacrine, quercetin, and tacrine-quercetin hybrid (Tac-Quer).

This work focuses on the combination of tacrine and quercetin to get a hybrid molecule (Fig. 1); tacrine as a cholinesterase inhibitor drug and quercetin as an antioxidant which is effective in metal depletion and reducing reactive oxygen species (ROS). This compound has been named Tac-Quer. It is very interesting that quercetin helps tacrine inhibit cholinesterase.

Initially, we evaluated the drug-likeness of Tac-Quer and its pharmacophores, namely tacrine and quercetin, individually with the aid of cApp software [46]. In this way, we determined Lipinski´s rule of five parameters for Tac-Quer, tacrine and quercetin. According to this rule, in general, drugs with a molecular weight (MWT) greater than 500 Daltons, a calculated log P greater than 5, more than 5 H-bond donors, and more than 10 H-bond acceptors were more likely to have poor absorption or permeation. Also, Veber *et al*. [47] suggested that compounds would have a high probability of good oral bioavailability if they had only two criteria: 10 or fewer rotatable bonds and a polar surface area equal to or less than 140 $Å^2$. All the parameters mentioned are calculated and listed in Table 1. Although the molecular weight of Tac-Quer was slightly higher than 500 D and its logP was higher than 5, the other parameters had suitable values. The desirable features included the presence of a sufficient number of hydrogen acceptors, aromatic system quantity, high volume, and topological polar surface area. Subsequently, the performance of the Tac-Quer ligand was evaluated.

The copper, iron, and zinc chelation activities of quercetin and Tac-Quer were investigated by quantum mechanics calculations. The inhibition of AChE and BChE by Tac-Quer was investigated employing molecular dynamic simulation as well. The results indicate that the combination of tacrine with quercetin leads to a new ligand that could simultaneously control some of the most important targets of Alzheimer's disease.

Table 1. The Calculated Lipinski´s Rule of Five Parameters for Three Ligands

Ligand name	Molecular mass (dalton)	logP[a]	H bond Don[b]	H bond Acc[c]	Rot. Bonds[d]	Ring Count[e]	T-PSA (Å)[f]
Tacrine	198.2	2.2	1	2	0	3	38.38
Quercetin	302.2	2.5	5	7	1	3	127.45
Tac-Quer	548.6	7.4	5	8	8	6	131.61

[a]Lipophilicity: logP is the logarithm of the partition coefficient (the ratio of the concentration of the ligand in octanol to its concentration in water). [b]Number of hydrogen bond donors. [c]Number of hydrogen bond acceptors. [d]Number of rotatable bonds. [e]Number of rings. [f]Topological polar surface area.

COMPUTATIONAL DETAILS

Quantum Mechanics Calculations

Geometry optimizations of the Tac-Quer/metal complexes were performed using the DFT/B3LYP method [48] with LANL2DZ [49] and 6-31G(d) basis sets for metal cations (Cu^{2+}, Zn^{2+} and Fe^{2+}) and for the other atoms, respectively. The quantum chemical calculations were carried out with the Gaussian 09 package [50]. In this study, frontier orbitals, HOMO-LUMO gap and MEP (molecular electrostatic potential) of Tac-Quer ligand and Tac-Quer/metal binding energy were calculated.

Preparation of the Initial Protein

The original crystallographic structures of the AChE and BChE enzymes were taken from the protein data bank (with the PDB ID of 2CKM and 4BDS, respectively). Since the polymorphism of AChE in the blood cells is often in a globular monomer form [51], only its asymmetric unit was used. For correct modeling of the enzyme's loops, a ModLoop server was used for adding the missing residues to the original enzyme structures [52,53]. The pKa values of the titratable residues obtained by the PROPKA web server and their surrounding environment were considered to assign the protonation state.

Docking Procedure

Docking calculations were done using the AutoDock Vina with default parameters. The grid box size was set at 47 × 47 × 47 Å (x, y and z) to include all the enzymes binding pocket. In order to appropriately fill the space between the CAS and PAS sites of AChE and BChE with a length of 14 Å, the number of carbon atoms between the tacrine and quercetin fragments was tested. The designed ligand with 4 to 7 carbon atoms between the two fragments was prepared for the docking process. The optimized ligands and repaired enzymes were used as the necessary input files for the docking studies. The enzymes and designed ligands structures were prepared using the AutoDockTools package (ADT; version 1.5.6) [54]. The details of assigning the protonation state to the titratable residues of both enzymes, merging the non-polar hydrogens to the optimized ligands, and dedicating the atomic charges to the ligand structure are available in Refs [55,56]. The docking results were evaluated *via* Accelrys Discovery Visualizer 3.5 [57]. Finally, the ligand with five carbon atoms was chosen as the final ligand (Fig. 1). Then, the stability of the selected ligand in the complex with the AChE and BChE enzymes was studied by MD simulation.

MD Simulations

MD simulations were carried out using the GROMACS MD package 5.0.7 [58] with an Amber99sb-ldn force field [59]. The AnteChamber PYthon Parser interfacE (ACPYPE) [60] and the general amber force field [61] were used to build the topological descriptions of the ligands. A water box with 12 Å distance from edges was utilized to prevent interactions of the protein with its own replicas. The modeled structures were solvated with the three-site TIP3P model. The systems were neutralized by adding 150 mM of NaCl. The LINCS algorithm and particle mesh Ewald (PME) algorithm were used to treat bonded and non-bonded

interactions. After minimizing the system by the steepest descent algorithm, the molecular dynamic simulations on the system were done under NVT ensemble, followed by employing the NPT ensemble (T = 300 K, P = 1 bar). The temperature and pressure coupling parameters were chosen to be $\tau t = 0.1$ ps and $\tau p = 0.5$ ps, respectively. All the NPT-MD simulations were performed for 20 ns using a 2 fs integration time step.

Protein-ligand Binding Free Energies

The protein-ligand complex binding free energies were calculated based on structural ensembles obtained from GROMACS trajectories [62,63] and derived from the following equation:

$$\Delta G_{binding} = G_{complex} - (G_{protein} + G_{ligand}) \quad (1)$$

$$G = U - TS = E_{MM} - TS_{MM} + G_{solv} \quad (2)$$

$$\Delta G_{binding} = \{\langle E_{MM}\rangle_{complex} - \langle E_{MM}\rangle_{protein} - \langle E_{MM}\rangle_{ligand}\} + \{\langle G_{solv}\rangle_{complex} - \langle G_{solv}\rangle_{protein} - \langle G_{solv}\rangle_{ligand}\} - T\{\langle S_{MM}\rangle_{complex} - \langle S_{MM}\rangle_{protein} - \langle S_{MM}\rangle_{ligand}\} \quad (3)$$

where $\langle E_{MM}\rangle$ is a molecular mechanics term (force field energy); $T\langle S_{MM}\rangle$ is conformational entropy; and $\langle G_{solv}\rangle$ includes polar and nonpolar solvation energy. The GROMACS tool GMXPBSA 2.1 [64] automatically calculated the binding free energies for the ligand-protein complexes.

In GMXPBSA [65], an Adaptive Poisson-Boltzmann Solver (APBS) electrostatics program was used for the calculation of the polar and nonpolar parts of the solvation energy. The calculations were performed on 250 frames of 20 ns trajectory. Furthermore, the water molecules were stripped out from the trajectory files to accelerate convergence by avoiding the solvent-solvent interactions in energy terms.

RESULTS AND DISCUSSION

Metal Chelating and Electronic Properties of Tac-Quer Ligand

As previously mentioned, metal ion imbalance is a significant factor in prodding and exacerbating of the multiple pathogens of AD. Quantum calculation was used to evaluate the metal chelating properties of the proposed ligand. In this study, the stability of Tac-Quer and metal complexes were examined. According to Eq. (4), the binding energy (BE) values are:

$$E\,(binding) = E\,(Tac\text{-}Quer\text{-}M\ complex) - E\,(M^{2+}) - E\,(Tac\text{-}Quer) \quad (4)$$

The amounts of binding energy listed in Table 2 obviously show that Tac-Quer has a high tendency to form a stable complex with all metal ions, showing the most tendency for Zn^{2+} followed by Cu^{2+} and Fe^{2+}.

The ability of the designed ligand to chelate metal ion was also compared to the quercetin molecule. Leopoldini *et al.* [40] also reported the binding energy for quercetin/iron complex. As seen in Table 2, the binding energies of the two molecules (Quercetin and Tac/Quer) with iron ion are in a similar range. These results confirmed that the quercetin fragment of the designed molecule maintained its ability to chelate metal ions. Therefore, it could act as a chelation agent and collect the extra metal ions from brain tissue, especially the copper ions that appear to be one of the main metal ions in plaque formation in AD.

In order to investigate the three-dimensional charge distribution of molecules, their molecular electrostatic potential (MEP) was calculated at the B3LYP/6-31G* optimized geometry (Fig. 2). This counter map helps to recognize and distinguish the nucleophilic and electrophilic reactive regions of the molecule that are essential for the proper study of the function of designed molecule in biological systems [66,67]. The MEP maps of tacrine and quercetin [68] are also shown for comparison.

The different colors show the different values of the electrostatic potential. The MEPs map of the Tac-Quer ligand shows that the oxygen and nitrogen atoms are located in negative regions, which are considered to be favorite sites for electrophilic attacks. These parts of the molecule interact with the AChE and BChE enzymes through hydrogen bonding, charge transfer, and π-π stacking. In the MEPs map, the most positive electrostatic potential (dark blue color) is on the hydrogen atoms attached to the oxygen atoms in phenyl groups. These regions are suitable sites for

Table 2. Binding Energy of Tac-Quer and Quercetin Ligands with Cu^{2+}, Zn^{2+} and Fe^{2+} Metal Ions Calculated Using Quantum Mechanics

Ligand name	Binding energy (kcal mol^{-1})		
	Cu^{2+}	Zn^{2+}	Fe^{2+}
Quercetin	- 837.87	- 859.69	- 610.23 (- 601.6 [40])
Tac-Quer	-917.62	- 939.08	- 694.103

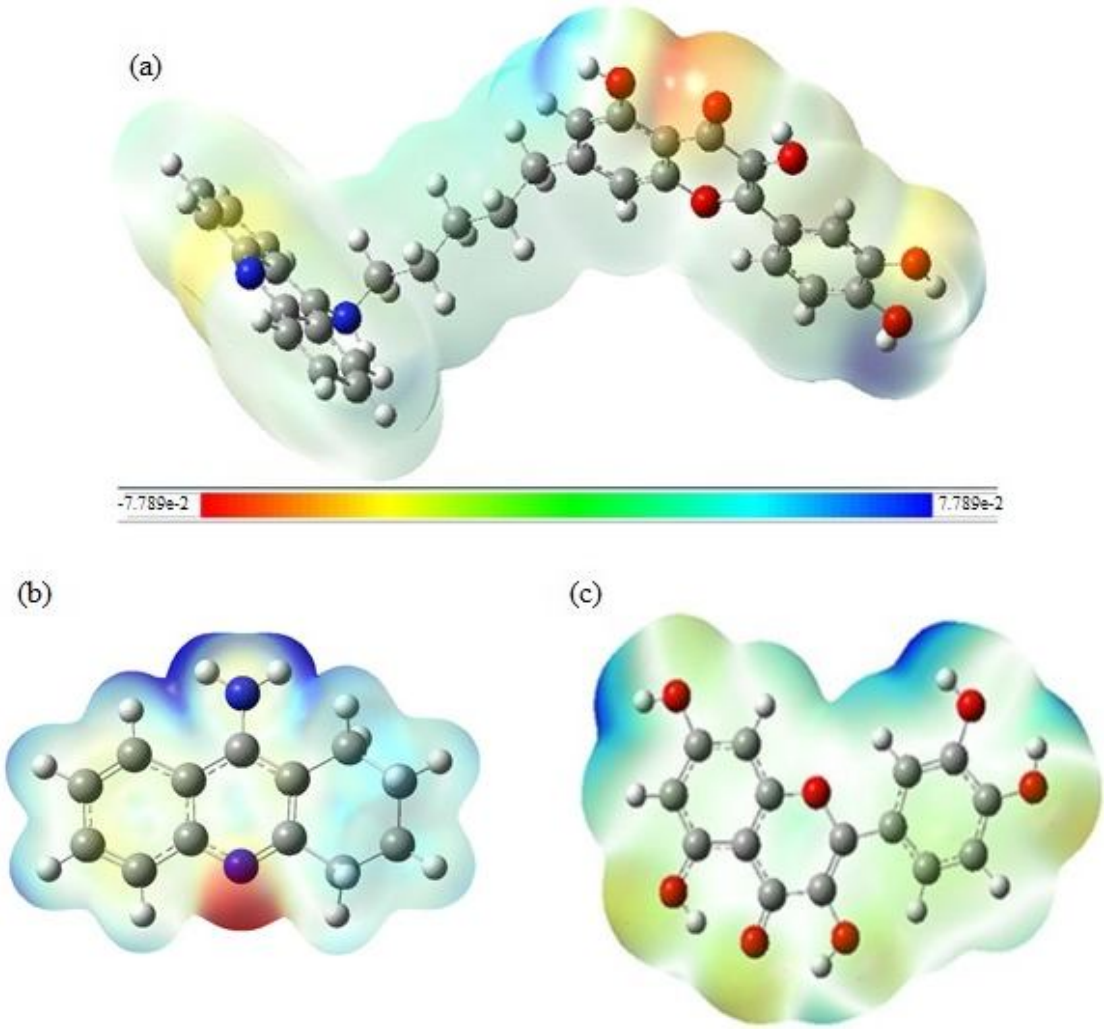

Fig. 2. MEP map of (a) tacrine-quercetin molecule, (b) tacrine molecule, and (c) quercetin molecule [68]. The different colors show the different values of the electrostatic potential. (negative regions: red color; positive regions: blue color).

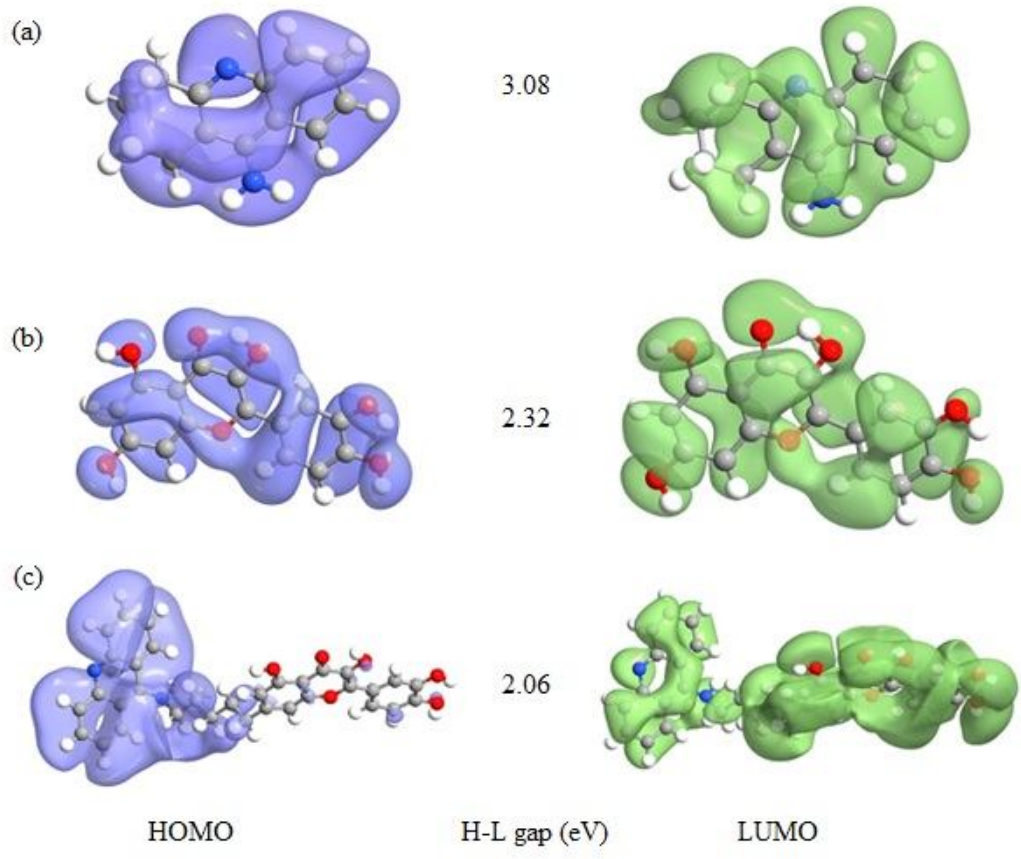

Fig. 3. Frontier molecular orbitals mapped on the optimized molecular structure of (a) tacrine, (b) quercetin and (c) Tac-Quervisualized using Virtual NanoLab (VNL) program.

nucleophilic attacks of AChE and BChE enzymes.

It is noteworthy that in metal chelation by the designed ligand, the negative regions play a major role. In the following, the electronic properties of the Tac-Quer molecule are studied using the energies of the highest occupied and the lowest unoccupied molecular orbitals (HOMO and LUMO, respectively). The contour plots of these orbitals are shown in Fig. 3. These orbitals are highly delocalized for Tac-Quer in comparison with tacrine and quercetin, which is one of the characteristics of the donor-acceptor systems. Both the HOMO and LUMO are delocalized in the tacrine and quercetin molecules. In the Tac-Quer molecule, LUMO is delocalized similar to its parent molecules, but HOMO is centered on the tacrine aromatic rings and nitrogen atoms. Thus, the electron pairs and π-electrons of tacrine region as a donor group can enhance its interaction with the acceptor and aromatic residues in the active sites of the AChE and BChE enzymes. As mentioned, the LUMO is delocalized over the entire molecule mainly distributed over the hydrogen atoms as electron acceptors.

The low amount of the Homo-Lumo gap confirms the high ability of the Tac-Quer ligand to form a stable complex with metal ions in comparison with its parents (tacrine and quercetin), especially quercetin which is a good chelator of metal ions. In order to understand the electronic properties of metal/Tac-Quer complexes, the distribution of HOMO and LUMO orbitals in optimized complexes are shown in Fig. 4. The highest LUMO distribution on the metal bonds with Tac-Quer is related to the Zn-complex, followed by copper and iron; this is related to the high tendency of the ligand to form a zinc complex. Regarding copper, the LUMO distribution is also very good to Cu-complex formation with Tac-Quer.

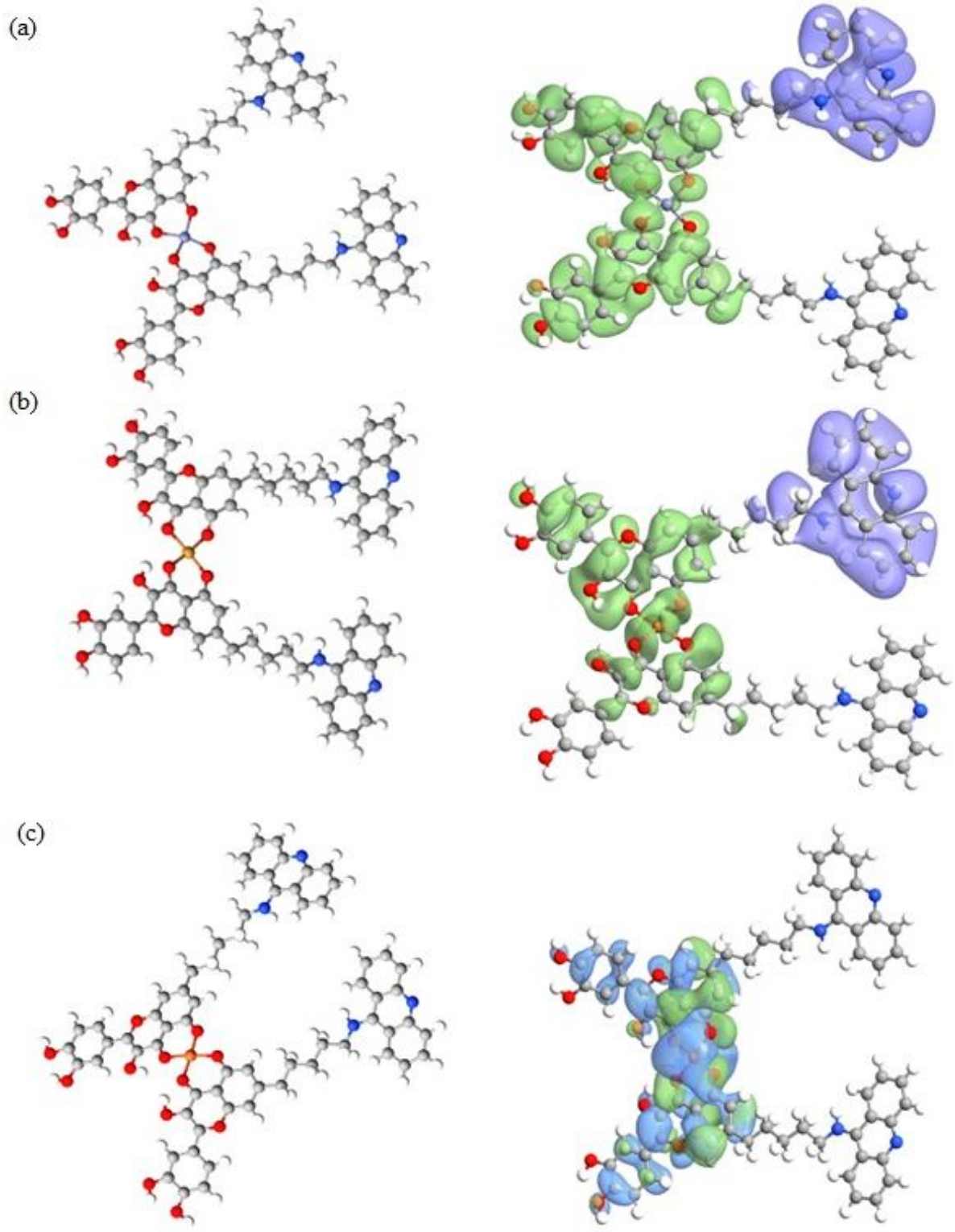

Fig. 4. Schematic structures of metal/Tac-Quer complexes and the distribution of frontier molecular orbitals mapped on the optimized structures. (a) Zn/Tac-Quer, Cu/Tac-Quer and (c) Fe/Tac-Quer.

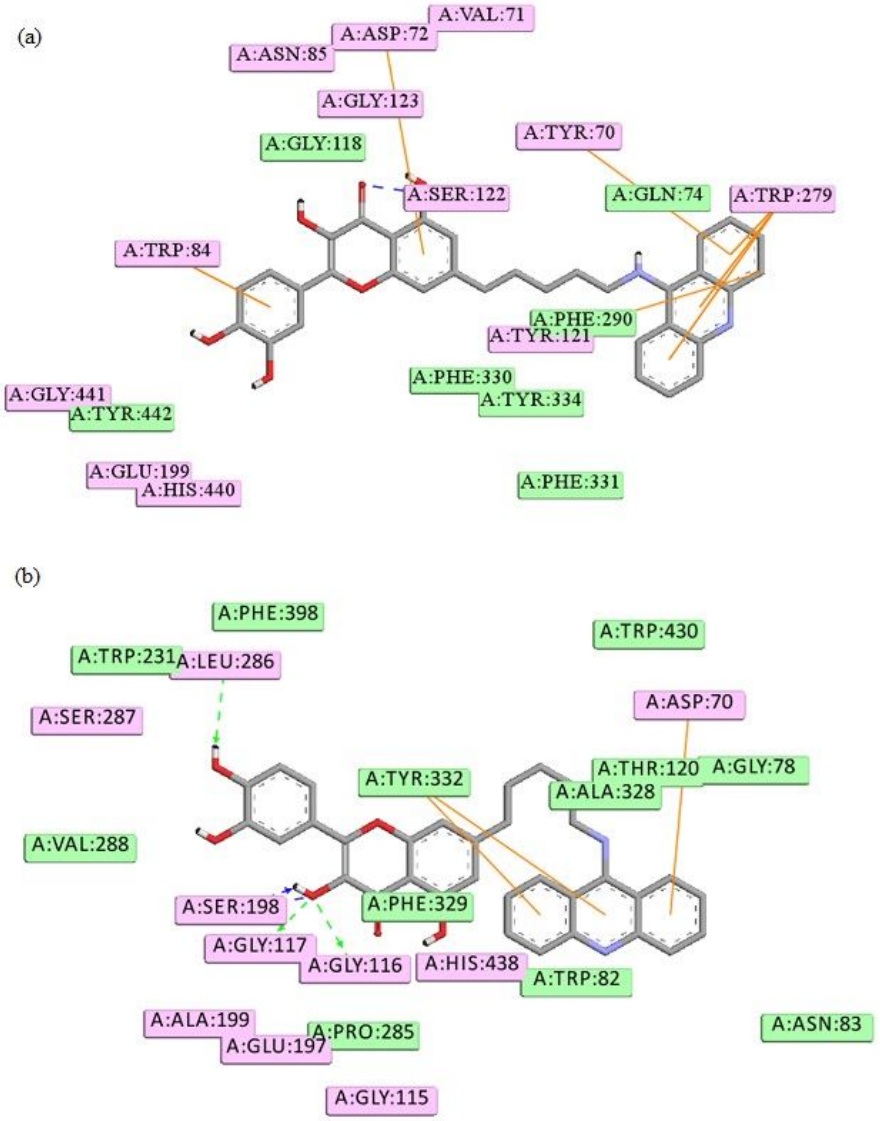

Fig. 5. Tac-Quer/enzymes interactions in Two dimension derived from molecular docking;: : van der Waals interaction, : electrostatic interaction, : π–π interaction; : hydrogen bond with amino acid side-chain; : hydrogen bond with amino acid main chain. (a) Tac-Quer/AChE complex, (b) Tac-Quer/BChE complex.

AChE and BChE Inhibition by Tac-Quer Ligand

To understand the Tac-Querligand/enzyme probable modes of interactions, we used molecular docking of the Tac-Quer ligand to AChE and BChE. Figure 5 shows two-dimensional representations of all interactions between the desired ligand and both enzymes. The docking results for the Tac-Quer ligand demonstrates that the residues of the catalytic sites of both enzymes interact with the quercetin fragment (His440 and Trp84 in AChE; Ser199, His438 and Trp82 in BChE), while the tacrine fragment establishes some interactions with the PAS residues of both enzymes (Tyr121, Trp279 and Tyr334 in AChE; Asp70 and Tyr332 in BChE). According to a study conducted on the tacrine molecule, this molecule only interacts with the important

residues of the choline-binding site (Catalytic Anionic Site or CAS) of both enzymes (Trp84 and Phe330 in the AChE and Trp82 of BChE) [69]. On this basis, it can be concluded that in a tacrine hybrid with quercetin, the quercetin fragment overcomes the tacrine for implantation in the CAS site. Since the PAS sites of both enzymes have more aromatic residues than the CAS (Trp84 and Phe330) and catalytic triad (Ser200, Glu327 and His440 of AChE and Ser199, Glu325 and His438 of BChE), this site is suitable for smaller fragments (tacrine). Actually, the size of the two fragments determines their location in the binding site of the enzymes. Since it is essential to prevent the formation of any form of toxic aggregated amyloid-beta by preventing the interactions of amyloid-beta monomers with the PAS site, the ability of Tac-Quer to inhibit PAS simultaneously with CAS is very valuable.

In order to evaluate the results of docking, the behavior and stability of the studied system are monitored and investigated during the MD simulation in this section. The two and three-dimensional representations of the Tac-Quer/Enzyme complexes at the end of the MD simulation time are shown in Figs. 6 and 7, respectively. The movements occurring during the MD simulation in both complexes represent the modification of the interactions between the proteins and the desired ligand. As mentioned above, Trp84 and Phe330 are two important residues of the AChE catalytic anionic site, while Trp82 and Ala328 are formed CAS in the BChE enzyme. These residues play a key role in the acetylcholine hydrolysis process.

The evaluation of the Tac-Quer/enzyme complexes at the end of the simulation time indicates that the quercetin fragment of the designed ligand has been placed near these residues; it interacts with AChE enzyme through π-π stacking electrostatic (Trp 84 residue), hydrophobic interactions (Phe330 residue), and hydrogen bonds (Trp 84 residue). In the interaction with BChE, π-π stacking electrostatic (Trp82 residue) and hydrophobic interactions (Ala328 residue) are also observed for the designed ligand. Among the residues in the peripheral anionic site (PAS) in AChE (typically, it includes Tyr70, Asp72, Tyr121, Trp279 and Tyr334 [70]), Trp279, Asp70 and Tyr70 have impressive interactions with the tacrine part of the ligand. In BChE, which usually has Asp70 and Tyr332 residues at PAS [70], the tacrine part of the ligand has an appropriate interaction with Tyr 332. In fact, the combination of tacrine and quercetin has led to the design of a new ligand that can engage all the important residues of the AChE and BChE enzymes.

The stability of the backbone atoms of both enzymes over the MD simulation has been investigated through the evaluation of the RMSD (root-mean-square deviation of atomic positions) plots. In Fig. 8a, insignificant fluctuation can be seen for the backbone atoms of both enzymes. On the other hand, the RMSD plot for the ligand molecule has also been investigated to monitor the ligand stability over the simulation time (Fig. 8b). The RMSD plot of tacrine-quercetin ligand in the Tac-Quer/BChE complex (Fig. 8b, red plot) does not show significant fluctuation. However, the RMSD plot of tacrine-quercetin ligand in the Tac-Quer/AChE complex ((Fig. 8b, blue plot) demonstrates a sudden increase up to the 3th ns in the RMSD value, even though this parameter has become almost stable from the 15th ns. These analysis plots along with the interaction detailes of ligand/anzymes (Figs. 5 and 6) derived from molecular docking and the MD simulation showed that the ligand displacement at the active sites of AChE was such that suitable interactions occurred and the Tac-Quer ligand was well sited on the active sites. Although the ligand movement in the active pathway of BChE was negligible (8b, red), examination of the interactions suggested that even this slight movement has led to improve the Tac-Quer/BChE interactions.

In the next step, the RMSF (root-mean-square fluctuation) parameter for all the residues of the AChE and BChE enzymes was investigated. It was seen that the oscillation of most of the AChE residues in the complex with the Tac-Quer ligand was insignificant and had the same value (Fig. 9a). Most of these residues were oscillating in the range of 0.05-0.4 nm. For the BChE enzyme, the range of residue oscillation was slightly higher (Fig. 9b), ranging from 0.05-0.4 nm. By examining the interactions at the end of the MD simulation, it was determined that BChE has more interaction with the Tac-Quer ligand than AChE. In fact, the oscillations of the BChE residues improved the Tac-Quer/BChE interactions. Moreover, the Dssp algorithm was used to evaluate the overall behavior of both enzymes [71]. As shown in Fig. 10a, the AChE enzyme in the Tac-Quer/AChE complex has an almost stable secondary

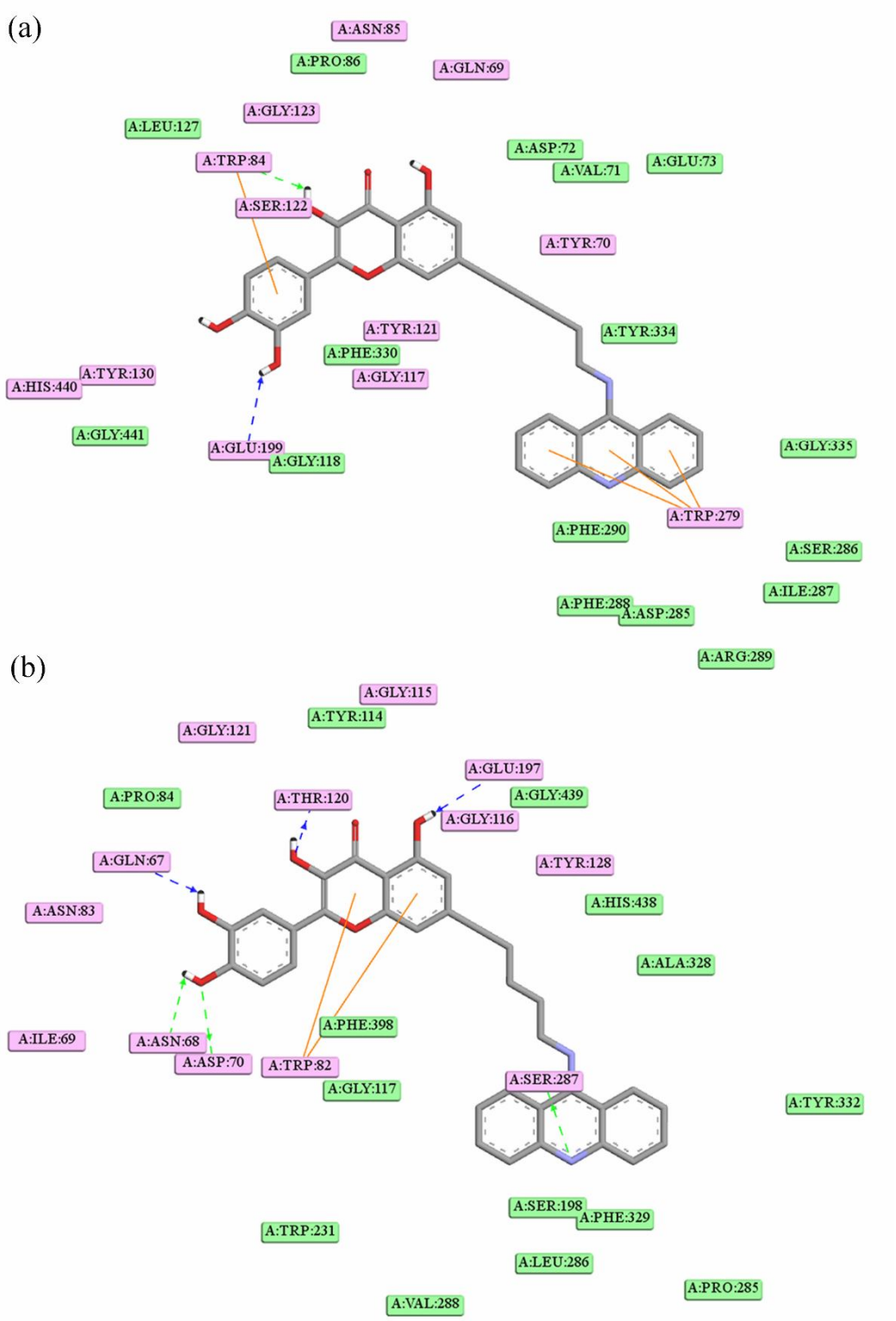

Fig. 6. Tac-Quer/enzymes interactions in two dimensions derived from molecular dynamic simulations; ▬: van der Waals interaction, ▬: electrostatic interaction, ▬: π-π interaction; - - - - - -: hydrogen bond with amino acid side-chain; - - - - - -: hydrogen bond with amino acid main chain. (a) Tac-Quer/AChE complex, and (b) Tac-Quer/BChE complex.

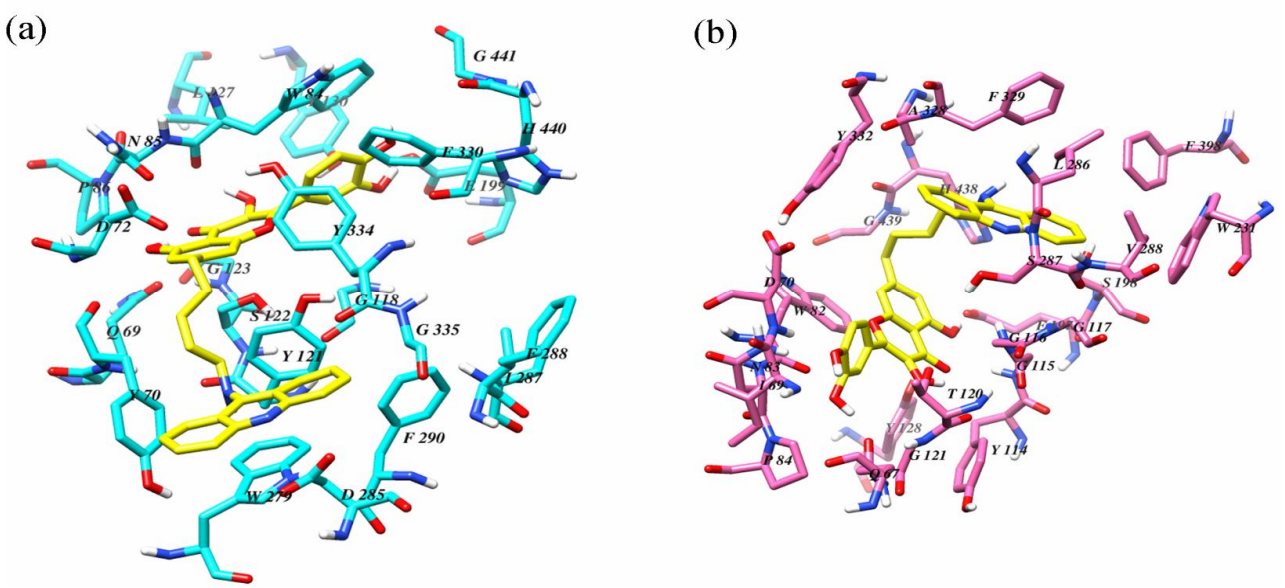

Fig. 7. Tac-Quer ligand (shown as sticks with yellow carbons) orientation at the active site of (a) AChE enzyme and (b) BChE enzyme in three dimentions derived from molecular dynamic simulations.

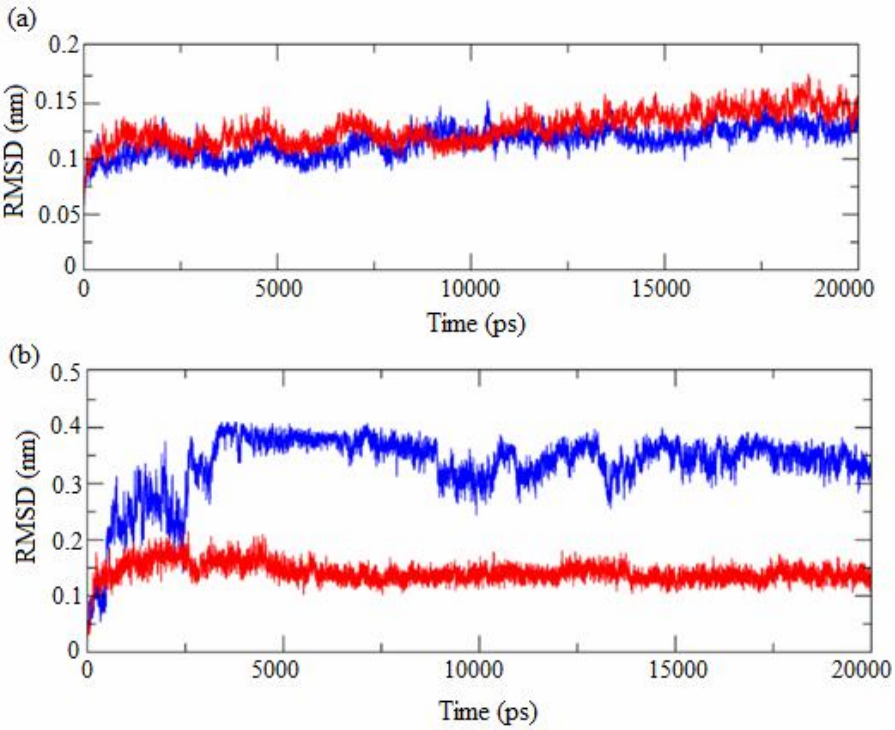

Fig. 8. (a) RMSD plots of the AChE (blue) and BChE (red) backbone atoms in Tac-Quer/AChE and Tac-Quer/BChE complexes, respectively. (b) RMSD plots of Tac-Quer ligand in Tac-Quer/AChE (blue) and Tac-Quer/BChE (red) complexes.

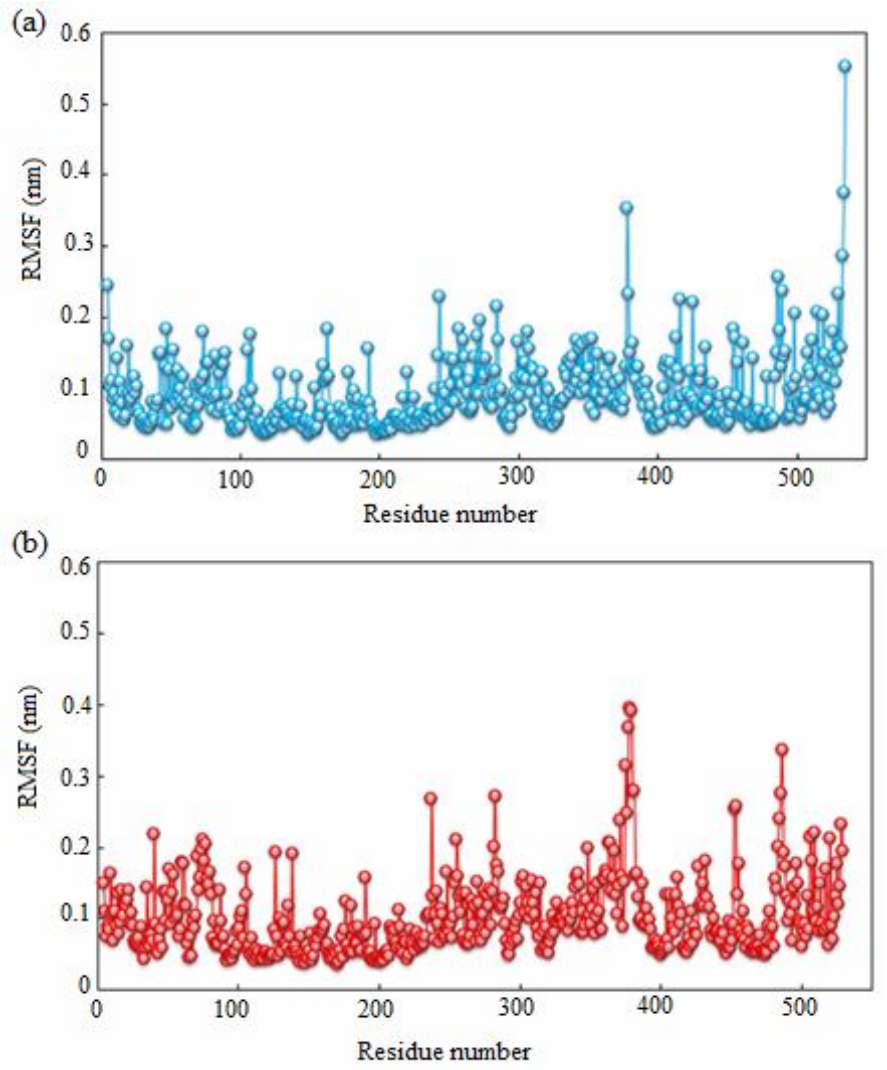

Fig. 9. RMSF plots of all residues of AChE enzyme in Tac-Quer/AChE complex (a), and BChE enzyme in Tac-Quer/BChE complex (b).

structure during the simulation time, while the BChE enzyme underwent some conformational changes in their secondary structure from the 18th ns (Fig. 10b). Actually, for BChE in the Tac-Quer/BChE complex, the number of residues with the 3-helix arrangement decreased during the MD simulation time while the number of residues with the α-helix arrangement increased.

Finally, free energy calculations were performed in order to verify the strength of the ligand inhibition. The results are reported in Table 3. In order to compare it with tacrine, a major reference source of free energy reported for this molecule is also presented in Table 3 [72]. It can be seen that in addition to filling the active site properly, the designed ligand has good inhibitory power. Even though, the evidence suggested a better BChE enzyme inhibition compared to AChE by this ligand. Thus, the higher hydrogen bond formed by the amino group of Tac-Quer with the catalytic triad of BChE could account for the higher potency of Tac-Quer against BChE in comparison with AChE.

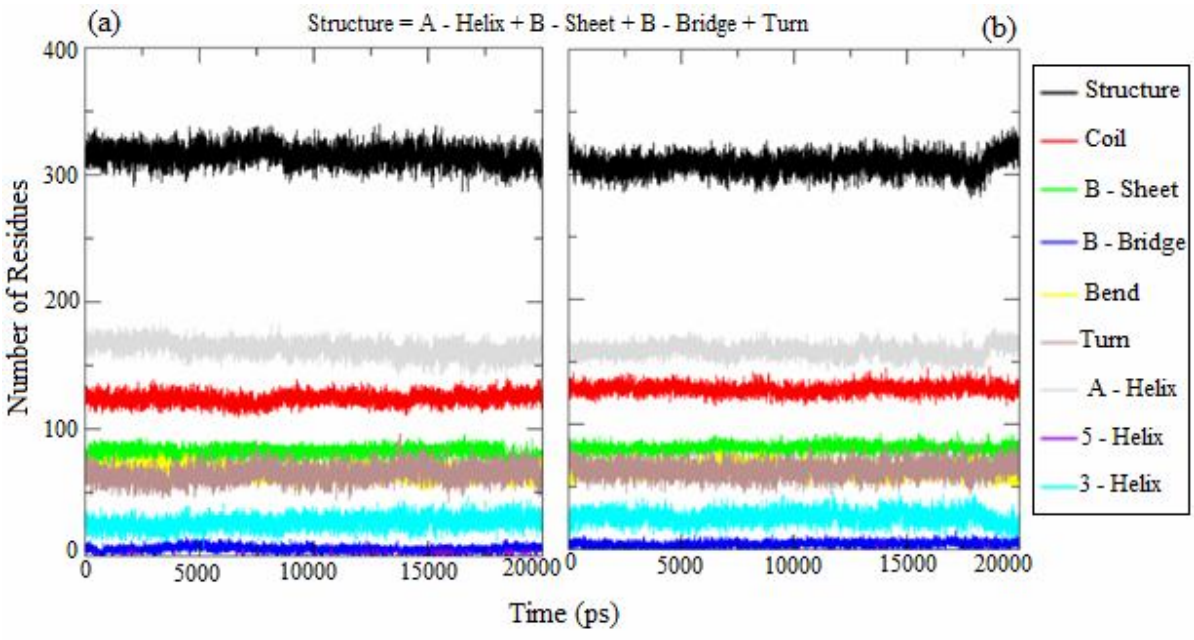

Fig. 10. (a) plot of AChE protein secondary structure in Tac-Quer/AChE complex, (b) plot of BChE proteinsecondary structure in Tac-Quer/BChE complex.

Table 3. Binding Free Energies for Protein-ligand Complexes Calculated with MM/PBSA Method for the MD Simulations (kcal mol^{-1})

Name of Complex	$\Delta G_{binding}$	
	Experimental	Computational
AChE-Tac	-10.2 [72]	-11.9 [72]
AChE/Tac-Quer	-	-17.17
BChE-Tac	-11.0 [72]	-13.4 [72]
BChE/Tac-Quer	-	-29.16

CONCLUSIONS

This study developed a new multi-target directed ligand (MTDL) for simultaneous control of the complex pathological conditions of Alzheimer's disease. In this approach, two distinct pharmacophores, namely tacrine, as a cholinesterase inhibitor drug, and quercetin, as an antioxidant, were combined in the same structure to get a hybrid molecule (Tac-Quer). Lipinski´s rule of five was applied to calculate the relevant parameters for Tac-Quer to evaluate its drug-likeness and bioavailability. Accordingly, Tac-Quer had a sufficient number of hydrogen acceptors, an aromatic system quantity, a high volume, a topological polar surface area, and consequently, a more likely high absorption or permeation. The study of the stability of the Tac-Quer/metal complexes revealed a very good ligand

strength to metallic ions chelating. The Tac-Quer/metal binding energies for Zn^{2+}, Cu^{2+} and Fe^{2+} were -939.08, -917.62 and -694.103 kcal mol^{-1}, respectively. Hence, Tac-Quer had a high tendency to form a stable complex with all metal ions, especially for Zn^{2+} and Cu^{2+}. The high tendency for Cu^{2+}, which is the main cationic element in plaque formation in AD, was one of the most powerful features of this ligand. The results of the molecular docking and molecular dynamics simulation showed that the appropriate ligand size, along with the presence of effective fragments (tacrine and quercetin), led to high ligand efficiency in blocking both the CAS and PAS sites of both the AChE and BChE enzymes and engaging with all their important residues. Based on the free energy calculations used to examine the strength of the ligand inhibition, it was seen that the designed ligand had good inhibitory power; it also had a better BChE enzyme inhibition compared to AChE. According to the results, the higher ability of the Tac-Quer ligand to inhibit BChE compared to AChE was related to the higher hydrogen bond formed by the amino group of Tac-Quer with the catalytic triad of BChE. In general, based on the results of the computational studies, it was found that the tacrine-quercetin hybrid has a good potential to prevent the onset and progression of AD.

ACKNOWLEDGMENTS

The authors are thankful to the Iranian Research Organization for Science and Technology (IROST) for their support in completing the present work.

REFERENCES

[1] Brookmeyer, R.; Johnson, E.; Ziegler-Graham, K.; Arrighi, H. M., Forecasting the global burden of Alzheimer's disease. *Alzheimer Dement.* **2007**, *3*, 186-191, DOI: 10.1016/j.jalz.2007.04.381.

[2] Townsend, M., When will Alzheimer's disease be cured? A pharmaceutical perspective. *J. Alzheimer. Dis.* **2011**, *24*, 43-52, DOI: 10.3233/JAD-2011-110020.

[3] Chopra, K.; Misra, S.; Kuhad, A., Neurobiological aspects of Alzheimer's disease. *Expert. Opin. Ther. Targets.* **2011**, *15*, 535-555, DOI: 10.1517/14728222.2011.557363.

[4] Marchbanks, R. M., Biochemistry of Alzheimer's dementia. *J. Neurochem.* **1982**, *39*, 9-15, DOI: 10.1111/j.1471-4159.1982.tb04695.x.

[5] Morphy, R.; Rankovic, Z., Designed multiple ligands. an emerging drug discovery paradigm. *J. Med. Chem.* **2005**, *48*, 6523-6543, DOI: 10.1021/jm058225d.

[6] Espinoza-Fonseca, L. M., The benefits of the multi-target approach in drug design and discovery. *Bioorg. Med. Chem.* **2006**, *14*, 896-897, DOI: 10.1016/j.bmc.2005.09.011.

[7] Querfurth, H. W.; LaFerla, F. M., Alzheimer´s disease. *N. Engl. J. Med.* **2010**, *362*, 329-344, DOI: 10.1056/NEJMra0909142.

[8] Bajda, M.; Guzior, N.; Ignasik, M.; Malawska, B., Multi-target-directed ligands in Alzheimer's disease treatment. *Curr. Med. Chem.* **2011**, *18*, 4949-75, DOI: 10.2174/092986711797535245

[9] Knez, D.; Coquelle, N.; Pišlar, A.; Žakelj, S.; Jukič, M.; Sova, M.; Mravljak. J.; Nachon, F.; Brazzolotto, X.; Kos, J.; Colletier, J. P.; Gobec, S., Multi-target-directed ligands for treating Alzheimer's disease: Butyrylcholinesterase inhibitors displaying antioxidant and neuroprotective activities. *Eur. J. Med. Chem.* **2018**, *156*, 598-617, DOI: 10.1016/j.ejmech.2018.07.033.

[10] Brown, J. H.; Laiken, N., Acetylcholine and Muscarinic Receptors, in: Robertson, D.; Biaggioni, I.; Burnstock, G.; Low, P. A.; Paton, J. F. R. (Eds.), Primer on the Autonomic Nervous System. Elsevier Inc: 2012, pp. 75-78.

[11] Mega, M. S., The cholinergic deficit in Alzheimer's disease: impact on cognition, behaviour and function. *Int. J. Neuropsychopharmacol.* **2000**, *3*, S3-S12, DOI: 10.1093/ijnp/3.supplement_2.s3.

[12] Greig, N. H.; Lahiri, D. K.; Sambamurti, K., butyrylcholinesterase: An Important new target in Alzheimer's disease therapy. *Int. Psychogeriatr.* **2002**, *14*, 77-91, DOI: 10.1017/S1041610203008676.

[13] Saxena, A.; Redman, A. M.; Jiang, X.; Lockridge, O.; Doctor, B. P., Differences in active site gorge dimensions of cholinesterases revealed by binding of inhibitors to human butyrylcholinesterase. *Biochem.* **1997**, *36*, 14642-51, 10.1021/bi971425.

[14] Dvir, H.; Silman, I.; Harel M.; Rosenberry, T. L.; Sussman, J. L., Acetylcholinesterase: From 3D structure to function. *Chem. Biol. Interact.* **2010**, *187*, 10-22, DOI: 10.1016/j.cbi.2010.01.042.

[15] Gupta, S.; Mohan, C. G., Dual binding site and selective acetylcholinesterase inhibitors derived from integrated pharmacophore models and sequential virtual screening. *Biomed. Res. Int.* **2014**, *2014*, 1-22, DOI: 10.1155/2014/291214.

[16] Carvajal, F. J.; Inestrosa, N.C., Interactions of AChE with Aβ Aggregates in Alzheimer's Brain: Therapeutic Relevance of IDN 5706. *Front. Mol. Neurosci.* **2011**, *4*, 1-10, DOI: 10.3389/ fnmol.2011.00019.

[17] Dinamarca, M. C.; Sagal, J. P.; Quintanilla, R. A.; Godoy, J. A.; Arrázola, M. S.; Inestrosa, N. C., Amyloid-β-Acetylcholinesterase complexes potentiate neurodegenerative changes induced by the Aβ peptide. Implications for the pathogenesis of Alzheimer's disease, *Mol. Neurodegener.* **2010**, *5*, 1-15, DOI: 10.1186/1750-1326-5-4.

[18] Barrow, C. J.; Small, D. H., Abeta Peptide and Alzheimer's Disease. Springer-Verlag, 2007.

[19] Maynard, C. J.; Bush, A. I.; Masters, C. L.; Cappai, R.; Li, Q. X., Metals and amyloid-b in Alzheimer's disease. *Int. J. Exp. Pathol.* **2005**, *86*, 147-159, DOI: 10.1111/j.0959-9673.2005.00434.x.

[20] Parthasarathy, S.; Yoo, B.; McElheny, D.; Tay, W.; Ishii, Y., Capturing a reactive state of amyloid aggregates: NMR-based characterization of copper-bound Alzheimer disease amyloid β-fibrils in a redox cycle. *J. Biol. Chem.* **2014**, *4*, 1-32, DOI: 10.1074/ jbc.M113.511345.

[21] Hu, D.; Serrano, F.; Oury, T. D.; Klann, E., Aging-dependent alterations in synaptic plasticity and memory in mice that overexpress extracellular superoxide dismutase. *J. Neurosci.* **2006**, *26*, 3933-3941, DOI: 10.1523/JNEUROSCI.5566-05.2006.

[22] Kishida, K. T.; Klann, E., Sources and targets of reactive oxygen species in synaptic plasticity and memory. *Antioxid. Redox. Signal.* **2007**, *9*, 233-244, DOI: 10.1089/ars.2007.9.233.

[23] Summers, W. K., Tacrine and Alzheimer's treatments. *J. Alzheimers. Dis.* **2006**, *9*, 439-446, DOI: 10.3233/ JAD-2006-9S350.

[24] Sameem, B.; Saeedi, M.; Mahdavi, M.; Shafiee, A., A review on tacrine-based scaffolds as multi-target drugs (MTDLs) for Alzheimer's disease. *Eur. J. Med. Chem.* **2017**, *128*, 332-345, DOI: 10.1016/ j.ejmech.2016.10.060.

[25] Li, W.; Mak, M.; Jiang, H.; Wang, Q.; Pang, Y.; Chen, K.; Han, Y., Novel anti-Alzheimer's dimer bis(7)-cognitin: cellular and molecular mechanisms of neuroprotection through multiple targets. *Neurotherapeutics*. **2009**, *6*, 187-201, DOI: 10.1016/ j.nurt.2008.10.040.

[26] Bolognesi, M. L.; Bartolini, M.; Mancini, F.; Chiriano, G.; Ceccarini, L.; Rosini, M.; Milelli, A.; Tumiatti, V.; Andrisano, V.; Melchiorre, C., Bis(7)-tacrine derivatives as multitarget-directed ligands: Focus on anticholinesterase and antiamyloid activities. *Chem. Med. Chem.* **2010**, *5*, 1215-1220, DOI: 10.1002/cmdc.201000086.

[27] Hiremathad, A.; Keri, R. S.; Esteves, A. R.; Cardoso, S. M.; Chaves, S.; Santos, M. A., Novel tacrine-hydroxyphenylbenzimidazole hybrids as potential multitarget drug candidates for Alzheimer's disease. *Eur. J. Med. Chem.* **2018**, *148*, 255-267, DOI: 10.1016/j.ejmech.2018.02.023.

[28] Hepnarova, V.; Korabecny, J.; Matouskova, L.; Jost, P.; Muckova, L.; Hrabinova, M.; Vykoukalova, N.; Kerhartova, M.; Kucera, T.; Dolezal, R.; Nepovimova, E.; Spilovska, K.; Mezeiova, E.; Pham, N. L.; Jun, D.; Staud, F.; Kaping, D.; Kuca, K.; Soukup, O., The concept of hybrid molecules of tacrine and benzyl quinolone carboxylic acid (BQCA) as multifunctional agents for Alzheimer's disease. *Eur. J. Med. Chem.* **2018**, *150*, 292-306, DOI: 10.1016/ j.ejmech.2018.02.083.

[29] Fang, L.; Jumpertz, S.; Zhang, Y.; Appenroth, D.; Fleck, C.; Mohr, K.; Tränkle, C.; Decker, M., Hybrid molecules from xanomeline and tacrine: enhanced tacrine actions on cholinesterases and muscarinic M1 receptors. *J. Med. Chem.* **2010**, *53*, 2094-2103, DOI: 10.1021/jm901616h.

[30] Fu, Y.; Mu, Y.; Lei, H.; Wang, P.; Li, X.; Leng, Q.; Han, L.; Qu, X.; Wang, Z.; Huang, X., Design, synthesis and evaluation of novel tacrine-ferulic acid

hybrids as multifunctional drug candidates against Alzheimer's disease. *Molecules.* **2016**, *21*, 1-10, DOI: 10.3390/molecules21101338.

[31] Zhu, J.; Yang, H.; Chen, Y.; Lin, H.; Li, Q.; Mo, J.; Bian, Y.; Pei, Y.; Sun, H., Synthesis, pharmacology and molecular docking on multifunctional tacrine-ferulic acid hybrids as cholinesterase inhibitors against Alzheimer's disease. *J. Enzyme. Inhib. Med. Chem.* **2018**, *33*, 496-506, 10.1080/14756366.2018.1430691.

[32] Xie, S. S.; Wang, X.; Jiang, N.; Yu, W.; Wang, K. D.; Lan, J. S.; Li, Z. R.; Kong, L. Y., Multi-target tacrine-coumarin hybrids: cholinesterase and monoamine oxidase B inhibition properties against Alzheimer's disease. *Eur. J. Med. Chem.* **2015**, *95*, 153-165, DOI: 10.1016/j.ejmech.2015.03.040.

[33] Hamulakova, S.; Janovec, L.; Soukup, O.; Jun, D.; Janockova, J.; Hrabinova, M.; Sepsova, V.; Kuca, K., Tacrine-coumarin and tacrine-7-chloroquinoline hybrids with thiourea linkers: Cholinesterase inhibition properties, kinetic study, molecular docking and permeability assay for blood-brain barrier. *Curr. Alzheimer. Res.* **2018**, *15*, 1096-1105, DOI: 10.2174/1567205015666180711110750.

[34] Camps, P.; El Achab, R.; Morral, J.; Muñoz-Torrero, D.; Badia, A.; Eladi Baños, J.; Vivas, N. M.; Barril, X.; Orozco, M.; Javier Luque, F., New tacrine-huperzine a hybrids (huprines): Highly potent Tight-binding acetylcholinesterase inhibitors of interest for the treatment of Alzheimer's disease. *J. Med. Chem.* **2000**, *43*, 4657-4666, DOI: 10.1021/jm000980y.

[35] Nepovimova, E.; Korabecny, J.; Dolezal, R.; Babkova, K.; Ondrejicek, A.; Jun, D.; Sepsova, V.; Horova, A.; Hrabinova, M.; Soukup, O.; Bukum, N.; Jost, P.; Muckova, L.; Kassa, J.; Malinak, D.; Andrs, M.; Kuca, K., Tacrine-trolox hybrids: A novel class of centrally active, nonhepatotoxic multi-target-directed ligands exerting anticholinesterase and antioxidant activities with low *in vivo* toxicity. *J. Med. Chem.* **2015**, *58*, 8985-9003, DOI: 10.1021/acs.jmedchem.5b01325.

[36] Spilovska, K.; Korabecny, J.; Sepsova, V.; Jun, D.; Hrabinova, M.; Jost, P.; Muckova, L.; Soukup, O.; Janockova, J.; Kucera, T.; Dolezal, R.; Mezeiova, E.; Kaping, D.; Kuca, K., Novel tacrine-scutellarin hybrids as multipotent anti-Alzheimer's agents: Design, synthesis and biological Evaluation. *Molecules.* **2017**, *22*, 1-22, DOI: 10.3390/molecules22061006.

[37] Li, X.; Wang, H.; Xu, Y.; Liu, W.; Gong, Q.; Wang, W.; Qiu, X.; Zhu, J.; Mao, F.; Zhang, H.; Li, J., Novel vilazodone-tacrine hybrids as potential multitarget-directed ligands for the treatment of Alzheimer's disease accompanied with depression: Design, synthesis, and biological evaluation. *ACS. Chem. Neurosci.* **2017**, *8*, 2708-2721, DOI: 10.1021/acschemneuro.7b00259.

[38] Liu, W.; Wang, H.; Li, X.; Xu, Y.; Zhang, J.; Wang, W.; Gong, Q.; Qiu, X.; Zhu, J.; Mao, F.; Zhang, H.; Li, J., Design, synthesis and evaluation of vilazodone-tacrine hybrids as multitarget-directed ligands against depression with cognitive impairment. *Bioor. Med. Chem.* **2018**, *26*, 3117-3125, DOI: 10.1016/j.bmc.2018.04.037.

[39] Panche, A. N.; Diwan, A. D.; Chandra, S. R., Flavonoids: an overview. *J. Nutr. Sci.* **2016**, *5*, 1-15, DOI: 10.1017/jns.2016.41.

[40] Leopoldini, M.; Russo, N.; Chiodo, S.; Toscano, M., Iron chelation by the powerful antioxidant flavonoid quercetin. *J. Agric. Food. Chem.* **2006**, *54*, 6343-6351, DOI: 10.1021/jf060986h.

[41] Aguirre, L.; Arias, N.; Teresa Macarulla, M.; Gracia, A.; Portillo, M. P., Beneficial effects of quercetin on obesity and diabetes. *Open. Nutraceuticals. J.* **2011**, *4*, 189-198, DOI: 10.2174/1876396001104010189.

[42] Zahedi, M.; Ghiasvand, R.; Feizi, A.; Asgari, G.; Darvish, L., Does quercetin improve cardiovascular risk factors and inflammatory biomarkers in women with Type 2 diabetes: A double-blind randomized controlled clinical Trial. *Int. J. Prev. Med.* **2013**, *4*, 777-785, PMID: 24049596.

[43] Gormaz, J. G.; Quintremil, S.; Rodrigo, R., Cardiovascular disease: A target for the pharmacological effects of quercetin, current topics in medicinal chemistry. *Curr. Top. Med. Chem.* **2015**, *15*, 1735-1742, DOI: 10.2174/1568026615666150427124357.

[44] Hashemzaei, M.; Delarami Far, A.; Yari, A.; Heravi,

R. E.; Tabrizian, K.; Taghdisi, S. M.; Sadegh, S. E.; Tsarouhas, K.; Kouretas, D.; Tzanakakis, G.; Nikitovic, D.; Anisimov, N. Y.; Spandidos, D. A.; Tsatsakis, A. M.; Rezaee, R., Anticancer and apoptosis-inducing effects of quercetin *in vitro* and *in vivo*. *Oncol. Rep*. **2017**, *38*, 819–828, DOI: 10.3892/or.2017.5766.

[45] Zhou, J.; Fang, L.; Liao, J.; Li, L.; Yao, W.; Xiong, Z.; Zhou, X., Investigation of the anti-cancer effect of quercetin on HepG2 cells *in vivo*. *PLoS. One.* **2017**, *12*, 1-10, DOI: 10.1371/journal.pone.0172838.

[46] Amani, P.; Sneyd, T.; Preston, S.; Young, N. D.; Mason, L.; Bailey, U. M.; Baell, J.; Camp, D.; Gasser, R. B.; Gorse, A. D.; Taylor, P.; Hofmann, A., A practical Java tool for small-molecule compound appraisal. *J. Cheminformatics.* **2015**, *7*, 1-4, DOI: 10.1186/s13321-015-0079-1.

[47] Veber, F. D.; Johnson, S. R.; Hung-Yuan, C.; Smith, B. R.; Ward, K. W.; Kopple, K. D., Molecular properties that influence the oral bioavailability of drug candidates. *J. Med. Chem*. **2002**, *45*, 2615-2623, DOI: 10.1021/jm020017n.

[48] Becke, A. D., A new mixing of Hartree-Fock and local density-functional theories. *J. Chem. Phys.* **1993**, *98*, 1372–1377, DOI: 10.1063/1.464304.

[49] Jeffrey Hay, P.; Wadt, W. A., *Ab Initio* effective core potentials for molecular calculations. Potentials for K to Au including the outermost core orbitals. *J. Chem. Phys.* **1985**, *82*, 298-310, DOI: 10.1063/1.448975.

[50] Frisch, M. J. *et al.,* Gaussian 09, Revision B. 01. Gaussian, Inc., 2009.

[51] Tripathi, A.; Srivastava, U. C., Acetylcholinesterase: A versatile enzyme of nervous system. *Ann. Neurosci.* **2010**, *15*, 106-111, DOI: 10.5214/ans.0972.7531.2008.150403.

[52] Fiser, A.; DO, R. K.; Sali, A., Modeling of loops in protein structures. *Protein. Sci.* **2000**, *9*, 175-177, DOI: 10.1110/ps.9.9.1753.

[53] Fiser, A.; Sali, A., ModLoop: automated modeling of loops in protein structures, *Bioinformatics.* **2003**, *19*, 2500-2501, DOI: 10.1093/bioinformatics/btg362.

[54] Morris, G. M.; Huey, R.; Lindstrom, W.; Sanner, M. F.; Belew, R. K.; Goodsell, D. S.; Olson, A. J., AutoDock4 and AutoDockTools4: Automated docking with selective receptor flexibility. *J. Comput. Chem*. **2009**, *30*, 2785-2791, DOI: 10.1002/jcc.21256.

[55] Wiesner, J.; Kříž, Z.; Kuča, K.; Jun, D.; Koča, J., Influence of the acetylcholinesterase active site protonation on omega loop and active site dynamics. *J. Biomol. Struct. Dyn.* **2010**, *28*, 393-403, DOI: 10.1080/07391102.2010.10507368.

[56] Trott, O.; Olson, A. J., AutoDock Vina: Improving the speed and accuracy of docking with a new scoring function, efficient optimization, and multithreading. *J. Comput. Chem.* **2010**, *31*, 455-461, DOI: 10.1002/jcc.21334.

[57] Accelrys Discovery Studio Visualizer v 3.5.: San Diego: Accelrys Software Inc., 2010.

[58] Abraham, M. J.; van der Spoel, D.; Lindahl, E.; Hess, B., GROMACS user manual version 5.0.7. the GROMACS development team, 2015, http://www.gromacs.org.

[59] Lindorff-Larsen, K.; Piana, S.; Palmo, K.; Maragakis, P.; Klepeis, J. L.; Dror, R. O.; Shaw, D. E., Improved side-chain torsion potentials for the Amber ff99SB protein force field. *Proteins.* **2010**, *78*, 1950-58, DOI: 10.1002/prot.22711.

[60] da Silva, A. W. S.; Vranken, W. F., ACPYPE-AnteChamber PYthon Parser interface. *BMC. Res. Notes.* **2012**, *5*, 1-8, DOI: 10.1186/1756-0500-5-367.

[61] Wang, J.; Wolf, R. M.; Caldwell, J. W.; Kollman, P. A.; Case, D. A., Development and testing of a General amber force field. *J. Comput. Chem.* **2004**, *25*, 1157-1174, DOI: 10.1002/jcc.20035.

[62] Kollman, P. A.; Massova, I.; Reyes, C.; Kuhn, B.; Huo, S.; Chong, L.; Lee, M.; Lee, T.; Duan, Y.; Wang, W.; Donini, O.; Cieplak, P.; Srinivasan, J.; Case, D. A.; Cheatham, T. E., Calculating structures and free energies of complex molecules: Combining molecular mechanics and continuum models. *Acc. Chem. Res.* **2000**, *33*, 889-897, DOI: 10.1021/ar000033j.

[63] Wang, J.; Morin, P.; Wang, W.; Kollman, P. A., Use of MM-PBSA in reproducing the binding free energies to HIV-1 RT of TIBO derivatives and predicting the binding mode to HIV-1 RT of efavirenz by docking and MM-PBSA. *J. Am. Chem. Soc.* **2001**, *123*, 5221-5230, DOI: 10.1021/ja003834q.

[64] Paissoni, C.; Spiliotopoulos, D.; Muscoa, G.; Spitaleri, A., GMXPBSA 2.1: A GROMACS tool to perform MM/PBSA and computational alanine scanning. *Comput. Phys. Commun.* **2015**, *186*, 105-107, DOI: 10.1016/j.cpc.2014.09.010.

[65] Paissoni, C.; Spiliotopoulos, D.; Muscoa, G.; Spitaleri, A., GMXPBSA 2.0: A GROMACS tool to perform MM/PBSA and computational alanine scanning. *Comput. Phys. Commun*. **2014**, *185*, 2920-2929, DOI: 10.1016/j.cpc.2014.06.019.

[66] Politzer, P.; Laurence, P. R.; Jayasuriya, K., Molecular electrostatic potentials: An effective tool for the elucidation of biochemical phenomena. *Environ. Health. Perspect.* **1985**, *61*, 191-202, DOI: 10.1289/ehp.8561191.

[67] Xavier, S.; Periandy, S.; Ramalingam, S., NBO, conformational, NLO, HOMO-LUMO, NMR and electronic spectral study on 1-phenyl-1-propanol by quantum computational methods. *Spectrochim. Acta. A. Mol. Biomol. Spectrosc*. **2015**, *137*, 306-320, DOI: 10.1016/j.saa.2014.08.039.

[68] Kumar, R.; Caruso, Í. P.; Ullah, A.; Cornélio, M. L.; Fossey, M. A.; Pereira de Souza, F.; Krishnaswamy Arni, R., Exploring the binding mechanism of flavonoid quercetin to phospholipase A2: Fluorescence spectroscopy and computational approach. *Euro. J. Exp. Bio*. **2017**, *7*, 1-10, DOI: 10.21767/2248-9215.100033.

[69] Eslami, M.; Hashemianzadeh, S. M.; Bagherzadeh, K.; Seyed Sajadi, S. A., Molecular perception of interactions between bis(7)tacrine and cystamine-tacrine dimer with cholinesterases as the promising proposed agents for the treatment of Alzheimer's disease. *J. Biomol. Struct. Dyn*. **2016**, *34*, 855-869, DOI: 10.1080/07391102.2015.1057526.

[70] Lane, R. M.; Potkin, S. G.; Enz A., Targeting acetylcholinesterase and butyrylcholinesterase in dementia. *Int. J. Neuropsychopharmacol.* **2006**, *9*, 101-124, DOI: 10.1017/s1461145705005833.

[71] Kabsch, W.; Sander, C., Dictionary of protein secondary structure: Pattern recognition of hydrogen-bonded and geometrical features. *Biopolymers.* **1983**, *22*, 2577-2637, DOI: 10.1002/bip.360221211.

[72] Sun, Q.; Peng, D. Y.; Yang, S. G.; Zhu, X. L.; Yang, W. C.; Yang, G. F., Syntheses of coumarin-tacrine hybrids as dual-site acetylcholinesterase inhibitors and their activity against butylcholinesterase, Ab aggregation, and b-secretase. *Bioorganic. Med. Chem.* **2014**, *22*, 4784-4791, DOI: 10.1016/ j.bmc.2014.06.057.